



## Simple approach for the synthesis of a 1,1'-(ethane-1,2-diylbis(azanediyl))bis(pentan-2-ol): $^{13}\text{C}/^1\text{H}$ NMR spectroscopy and electrical characterizations

Lassaad Wechteti<sup>\*a</sup>, Ahmed Souemti<sup>b</sup>, Aymen Selmi<sup>c</sup> & Moufida Romdhani-Younes<sup>a</sup>

<sup>a</sup>University of Tunis El Manar, Faculty of Sciences of Tunis, Chemistry Department, Laboratory of Structural Organic Chemistry, 2092 Tunis, Tunisia

<sup>b</sup>University of Tunis El Manar, Faculty of Sciences of Tunis, Chemistry Department, LR19ES02 Applied Mineral Chemistry Laboratory (LCMA), 2092 Tunis, Tunisia

<sup>c</sup>University of Tunis El Manar, Faculty of Sciences of Tunis, Physics Department, LR99ES17 Laboratory of Materials Organisation and Properties, 2092 Tunis, Tunisia

E-mail: lwechteti@yahoo.fr

Received 27 September 2021; accepted (revised) 24 February 2022

1,1'-(Ethane-1,2-diylbis(azanediyl))bis(pentan-2-ol) a  $\beta$ -aminoalcohol material denoted as **2a** has been successfully synthesized. A white highly pure transparent material has been obtained after purification by chromatography techniques. Infrared spectroscopy has been used to identify the  $-\text{NH}$  and  $-\text{OH}$  functional groups.  $^1\text{H}$  and  $^{13}\text{C}$  NMR spectroscopy has confirmed the proposed structure. Complex Impedance Spectroscopy indicates an insulator behavior of the studied materials in the 313-393°C temperature range. Conductivity within this material is in intragrain contribution and its activation energy is about 1.3 eV. The physical properties of the studied material allow to consider  $\beta$ -amino alcohols as versatile intermediates for many organic compounds in the making of natural and synthetic originated biologically active compounds. They are widely used as  $\beta$ -blockers, insecticidal agents, and chiral auxiliaries.

**Keywords:**  $\beta$ -Aminoalcohols, vibrational modes, activation energy, Arrhenius plot, dielectric properties

Organic synthesis has undergone great development in recent years due to the modification of the classical synthesis methodologies and the use of new reaction processes, catalysts, and solvents. These reactions have become more efficient and less expensive<sup>1-3</sup>. In this context, the development of simple, efficient, and easy-to-implement processes for the preparation of amino alcohols, especially the opening of epoxides by amines, represents a major challenge in modern chemistry<sup>4</sup>. Epoxides (oxacyclopropanes or oxiranes) are organic compounds in which the oxygen is located (in the form of a bridge) on a carbon-carbon link. They are mediators key for organic synthesis, due to their reactivity towards nucleophiles by giving heteroatomic products on the one hand<sup>5</sup> and their use in synthesizing of many biologically active compounds, such as antibiotics (Mupirocin: Antibiotic of natural origin on the other hand<sup>6</sup>). Generally, the synthesis of an attack of a nucleophile (amine group) on the epoxides at high temperature. on the other side, some  $\beta$ -amino alcohols are obtained from trifluoromethyloxirane as indicated

by Coudures<sup>7</sup>. In summary, these materials are very interesting compounds, either their use as ligands for asymmetric catalysis<sup>8</sup> or the preparation of biologically active molecules<sup>9</sup>. Aromatic and heteroaromatic amino alcohols have been synthesized by Almeida's team<sup>10</sup> and the obtained results show a better activity against bacteria when evaluated by the agar diffusion method and have been selected for the evaluation of the minimum inhibitory concentrations. Another important type of amino alcohols are those that carry a free amine group and are used in different protector group strategies (e.g. N-Boc or NF-moc) or in the synthesis of biomolecules that can be the starting materials for the preparation of important types of catalytic ligands such as oxazaborolidines<sup>11,12</sup>, bis(oxazolines)<sup>13</sup>, or phosphinoxazolines<sup>14-16</sup>. These molecules are also known as  $\beta$ -blockers, they are used in the treatment of cardiovascular disorders and oppose the  $\beta$ -adrenergic of catecholamines<sup>17</sup>. They are also involved in several electrochemical processes<sup>18-21</sup>, industrial<sup>22</sup>, related to the many pathways of heterocycles<sup>23-26</sup>. The

physical properties of  $\beta$ -amino alcohols have not been studied before. In this work, we are interested in the synthesis of material of this family and we will then study its electrical and dielectric properties.

### Experimental Section

$^1\text{H}$  and  $^{13}\text{C}$  NMR spectra were recorded on a Bruker AC 300 spectrometer at 300 and 75 MHz, respectively in  $\text{CDCl}_3$  (TMS). The Fourier transform infrared spectrum was recorded using a Nicolet IR 200 FT-IR spectrometer in the  $1400\text{--}400\text{ cm}^{-1}$  range. The electric and dielectric measurements were performed with a Solartron SI 1260 Impedance Analyzer coupled to a Dielectric Interface 1296 in the  $10^2\text{ Hz} - 10^6\text{ Hz}$  frequency range.

### Synthetic procedure

A general procedure is used for the synthesis of 1,1'-(ethane-1,2 diylbis(azanediyl))bis(pentan-2-ol): A solution of ethylenediamine (5 mmol) in ethanol (5 mL) was added to a solution of 2-butyloxirane **1a** (10 mmol) in ethanol (10 mL), drop-wise while stirring at RT for about 15 min. The progress of the reaction was monitored by TLC eluant: cyclohexane/ethyl acetate: 8/2). After completion of the reaction, the mixture was diluted with water (15 mL) and the product was extracted with diethyl ether ( $3 \times 20\text{ mL}$ ). The organic extracts were dried over anhydrous sodium sulfate and concentrated under reduced pressure. The crude product was purified by chromatography column on silica gel (cyclohexane/ethyl acetate: 8/2) to get pure compounds **2a** with a yield of 89%. The proposed reaction as follows (Scheme I).

### Results and Discussion

#### FT-IR spectroscopy

FT-IR spectrum registered in the frequency range  $500\text{--}3500\text{ cm}^{-1}$  of **2a** material is given in Figure 1. The obtained result confirms the purity of the obtained phase. Indeed, on the spectrum appears the relative bands of vibrational modes of the NH and OH groups present in the formula of the product. Several bands are considered on the spectrum of which we

note among them: first, the two absorption bands located at  $3120$  and  $3288\text{ cm}^{-1}$  are attributed to the vibrational modes of the NH and OH bonds. Second, the absorption band located around  $2851\text{ cm}^{-1}$  corresponds to the vibration of the  $\text{CH}_2\text{NH}$  group. Third, at  $2928\text{ cm}^{-1}$  is located the band related to the vibration of the asymmetric carbon. Finally, the alkyl group (Butyl) appears between  $1477$  and  $809\text{ cm}^{-1}$ .

#### $^1\text{H}$ NMR spectroscopy

The  $^1\text{H}$  NMR spectrum of **2a** sample is presented in Figure 2. Indeed, we notice the disappearance of the protons signals at around 2.54 ppm and the appearance of new signals corresponding to the protons carried by the carbon bound of the amine function  $\text{CH}_2\text{NH}$  and the proton carried by the carbon which carries the alcohol  $\text{CHOH}$ . The  $^1\text{H}$  NMR spectrum also confirms that the molecule is symmetrical. A single singlet is located at  $\delta = 2.77$  ppm corresponds to the two methylene groups  $\text{NCH}_2\text{CH}_2\text{N}$ . In addition, the triplet corresponds to the two  $\text{CH}_3$  groups is observed at around  $\delta 0.94$ . The two protons' amine groups appear as broadband at  $\delta 3.14$ . The protons of the two  $-\text{CH}_2-\text{CH}_2-\text{CH}_2-$  in  $\alpha$ -group of the alcohol function appear as multiplets at 1.33 to 1.49 ppm. The protons of the two  $\text{CH}_2$  groups in  $\alpha$  of amine NH and  $\beta$  of alcohol appear in ABX system at 2.51 to 2.68 ppm. A multiplet of 3.65 to 3.70 ppm

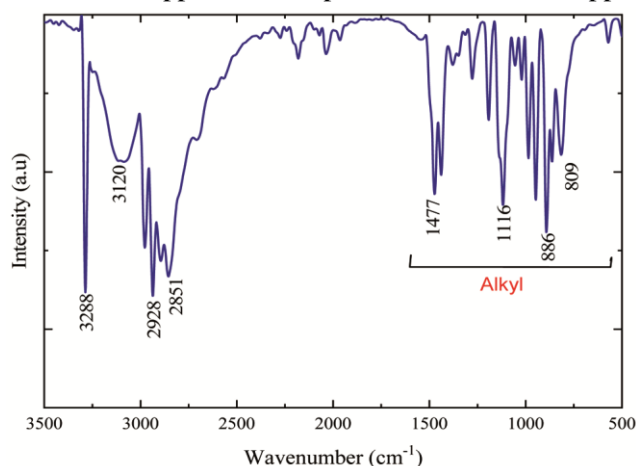
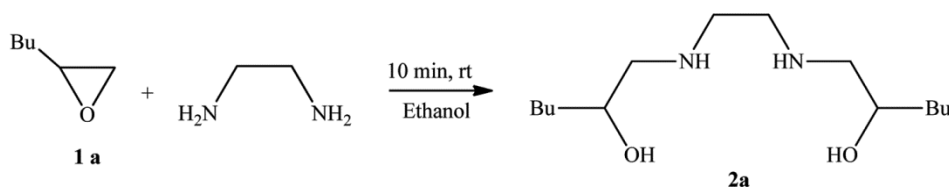
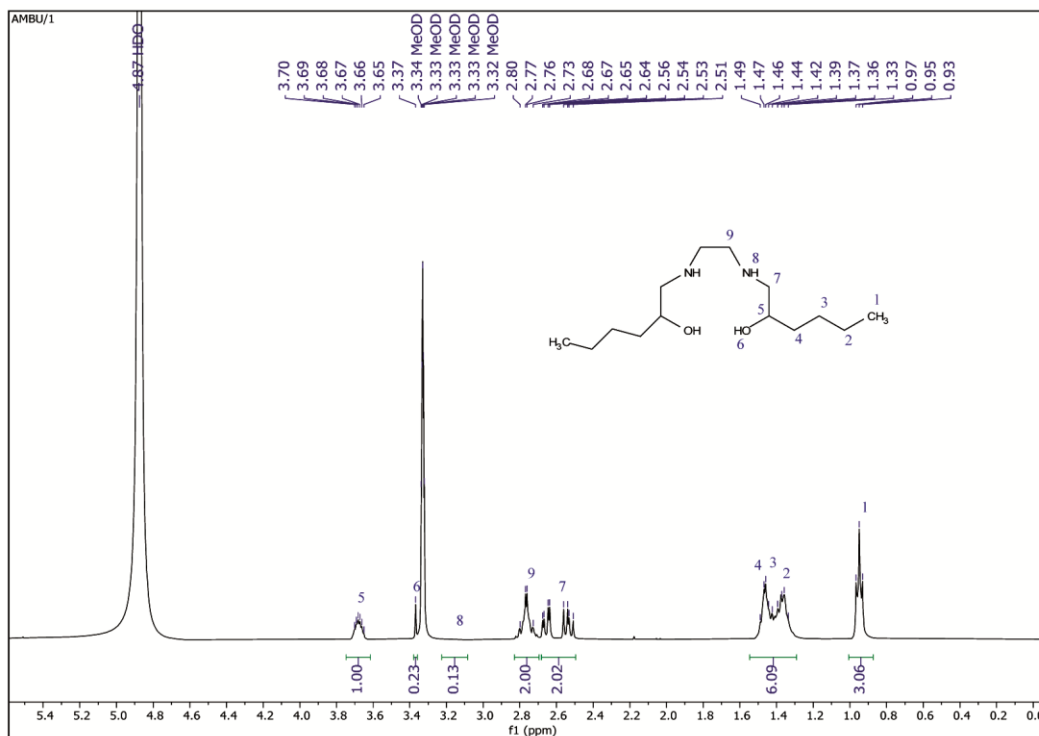


Figure 1 — IR spectrum of the **2a** material



Scheme I

Figure 2 —  $^1\text{H}$  NMR spectrum of **2a** material

relative to the two protons carried by the asymmetric carbon. The two protons of the two alcohol functions are in the form of broadband at 3.37 ppm.

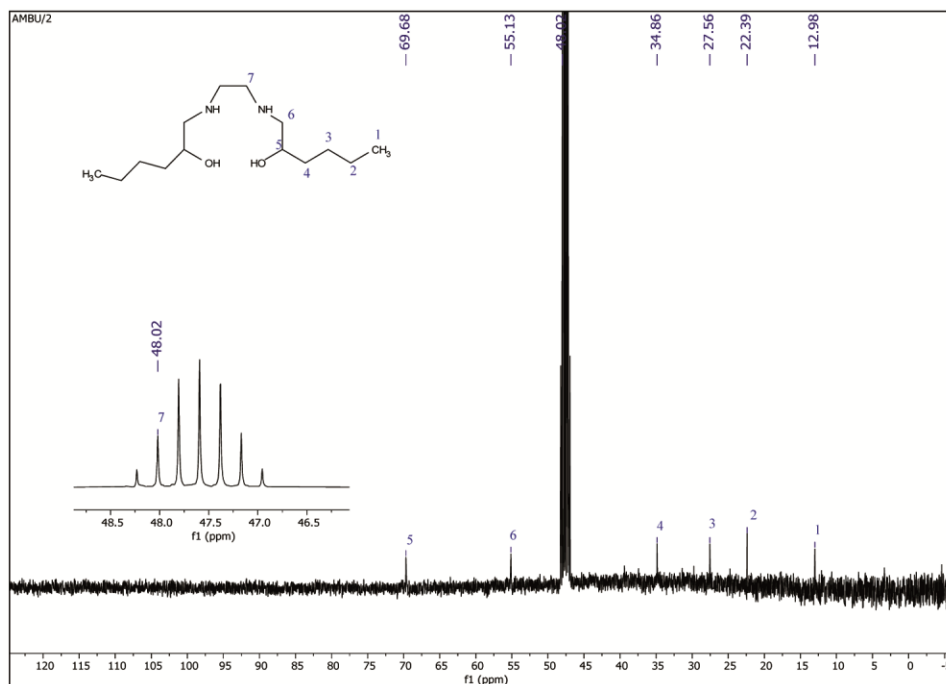
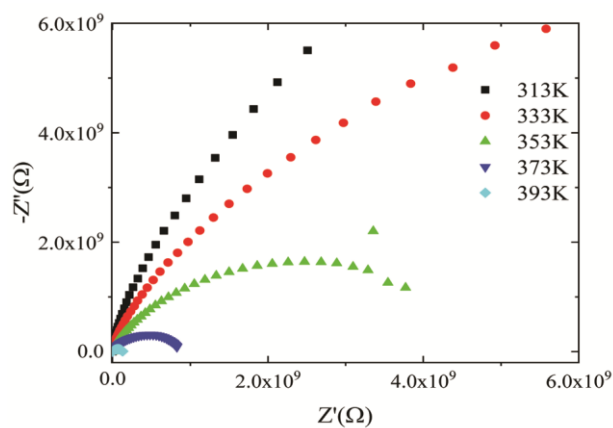
### $^{13}\text{C}$ NMR spectroscopy

The uncoupled  $^{13}\text{C}$  NMR spectrum of the proton of amino alcohol **2a** is in good agreement with the proposed structure and also shows that this molecule is symmetrical. Besides the signals relating to the carbon atoms of the alkyl groups, three different signals are corresponding to the six aliphatic carbon atoms. We detail the spectral data of compound **2a** reproduced in Figure 3, and which shows peaks characteristic of asymmetric carbon directly linked to the alcohol function and in  $\beta$  of the amine group which resonates around 69.68 ppm and of carbon in  $\beta$  of the hydroxyl group and  $\alpha$  of the amine group resonating at around 55.13 ppm. On this spectrum also appears: A signal at around 48.02 ppm relating to the carbon of the  $\text{CH}_2$  group in  $\alpha$  of the amine group. Signals around 12.98; 22.39; 27.56; 34.86 ppm relating to the alkyl groups.

### Electrical properties of **2a** material

The study of the dielectric properties of materials is an essential parameter for integrating these materials

into microelectronic application devices. The dielectric properties of the **2a** material were measured as a function of frequency ( $10^{-1}$  Hz to  $10^6$  Hz) and temperature ( $25^\circ\text{C}$ - $300^\circ\text{C}$ ). Indeed the compound is stable in this range and does not undergo any decomposition. A pellet of the material was prepared under a pressure of  $5 \text{ tons.cm}^{-1}$  and then sintered at 373 K. In order to separate and identify the contribution of the electrode effects, grain boundaries, and grain on the phenomenon of charge transport in our products, we have adopted the complex impedance method ( $Z'' = f(Z')$ ). The Nyquist diagrams of the prepared pellet, showing the variation of the imaginary part  $Z''$  as a function of the real part  $Z'$  of the impedance are shown in Figure 4. It is observed from the figure that only single semi-circles are present indicating that the electric conduction is done in volume and through the grains<sup>27</sup>. Moreover, the total resistance of the material is given by the intersection of semicircles with the  $Z'$  axis. The values of resistance and conductivity observed in Table I are in the order of  $10^{-10} \Omega$ , which indicates an insulating character of the studied material. On the other hand, this resistance decreases when the temperature increases suggesting a thermally activated mechanism process. The values of conductivity on each temperature is calculated using the equation<sup>28-30</sup>:

Figure 3 —  $^{13}\text{C}$  NMR of **2a** materialFigure 4 — Nyquist diagrams of **2a** material

$$\sigma = \frac{\epsilon}{R.S} \quad \dots(1)$$

Figure 5 depicts the variation of the total conductivity  $\sigma$  within the studied material. It is well observed that it is thermally activated. It decreases when temperature increases. This behaviour is linear and follows the Arrhenius law. The Arrhenius law in such a thermally activated system is given by the following relation<sup>31,32</sup>:

$$\sigma.T = A.e^{\frac{-E_a}{K_B T}} \quad \dots(2)$$

Where  $\sigma$ , T, A,  $K_B$  and  $E_a$  are the conductivity ( $\text{S.cm}^{-1}$ ), absolute temperature (K), a pre-exponential

Table I — Resistance and conductivity values as function of temperature for **2a** sample

T (K)	R ( $10^9 \Omega$ )	$\sigma$ ( $10^{-11} \text{ S.cm}^{-1}$ )
313	25.31	0.62
333	10.62	1.49
353	3.24	4.77
373	0.47	33.11
393	0.071	220.57

factor, the Boltzmann constant, and the activation energy (eV), respectively.

The activation energy is deduced from the slope of Figure 6 and its value equal to 1.29 eV.

Dielectric materials are non-conducting substances. They are the insulating materials and are bad conductors of electric current. Dielectric materials can hold an electrostatic charge while dissipating minimal energy in the form of heat. Examples of dielectric are plastics, glass, porcelain, and various metal oxides. In our case, the study of dielectric properties of **2a** materials is based essentially on the behavior of the real part  $\epsilon'$ , the imaginary part  $\epsilon''$ , and loss factor  $\tan \delta$  of the permittivity of the material as a function of frequency.

The expressions of  $\epsilon'$ ,  $\epsilon''$ , and  $\tan \delta$  are given by<sup>30</sup>:

$$\epsilon'(\omega) = -\frac{Z''}{\omega C_0(Z'^2 + JZ''^2)} \quad \dots(3)$$

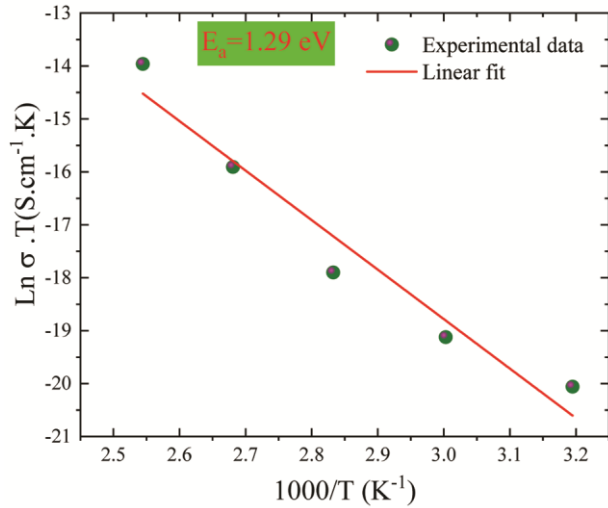


Figure 5 — Arrhenius plot of **2a** material

$$\epsilon'(\omega) = \frac{Z'}{\omega C_0 (Z'^2 + JZ''^2)} \quad \dots(4)$$

$$\text{Tang } \delta = \frac{\epsilon''}{\epsilon'} \quad \dots(5)$$

Where  $Z'$  is the real part of impedance;  $Z''$  is its imaginary part.

$C_0 = \frac{\epsilon_0 A}{e}$ :  $\epsilon_0$  is the permittivity of the vacuum equal to  $8.854 \cdot 10^{-12} \text{ Fm}^{-1}$ ;  $A$  is the cross-sectional area of the flat surface of the pellet ( $75.2 \cdot 10^{-6} \text{ m}^2$ ),  $e$  is its thickness (2 mm). Frequency dependence of  $\epsilon'$ ,  $\epsilon''$ , and  $\tan \delta$  as a function of temperature is given in Figure 6a-c. It is seen from the figure that the dielectric parameters decreased sharply with frequency up to a certain critical value, and then remained constant. The shape of the dielectric characteristics is the result of the inhomogeneous nature of the dielectric structure. The variation of the dielectric constant with frequency reveals dispersion due to Maxwell-Wagner type interfacial polarization<sup>30</sup>. The dependence on the frequency of a dielectric at low frequencies can result from build-ups of charge. This polarization occurs at the grain boundaries in a way that causes a separation of charges by a considerable distance from which the dielectric loss becomes very important<sup>33</sup>. As frequency increases, the jump frequency of the charge carriers can not follow the oscillation of the applied electric field, and thus the different types of polarization decrease and finally disappear. This is why the permittivity decreases by increasing the frequency<sup>33</sup>. The large values of the dielectric constant at low frequencies are mainly due to the presence of different types of polarization including

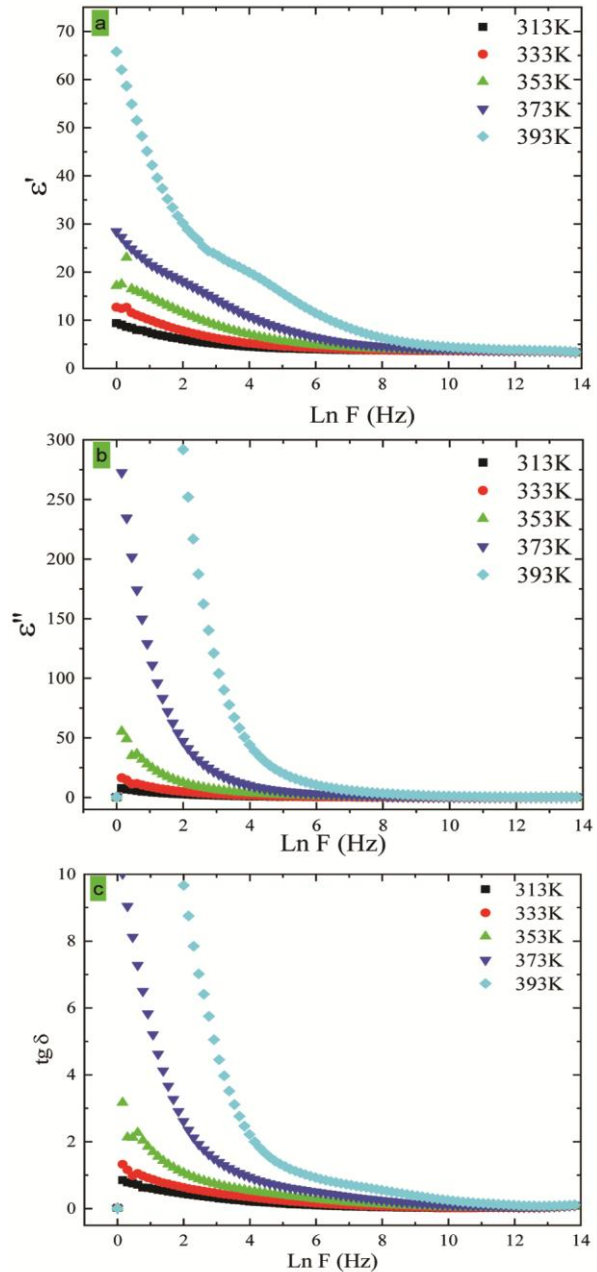


Figure 6 — The frequency dependence curves of dielectric constant  $\epsilon'(\omega)$  (a),  $\epsilon''(\omega)$  (b) and loss factor (c) for **2a** material

electronic, dipolar, and spatial charge contributions<sup>33</sup>. In addition, these values can be explained by transitions of charge carriers from one site to another that requires higher energy. The main contribution in low-frequency comes from the grain boundaries where the energy loss is very high and corresponds to high resistances. Thus, the low permittivity values presented low-k material can be used as insulators between metallic interconnections to reduce the coupling between them.

## Conclusion

A facile organic synthesis is used for the elaboration of **2a**  $\beta$ -alcohol material. A high purity compound was obtained. Asymmetric compound and a specific structure were determined utilizing NMR of  $^1\text{H}$  and  $^{13}\text{C}$ . The analysis by IR spectroscopy confirmed the presence of vibrational modes related to X-H links (X=O; N). The impedance spectroscopy analysis suggesting an insulator character for the studied material. With its high value of activation energy ( $E_a=1.29$  eV) in the [313-393 K] temperature range, **2a** material has a low conductivity value from the bulk contribution. The obtained low permittivity values allow classifying this material as low-k material which can be used as versatile intermediate in the preparation of many biologically active compounds as well as in the pharmaceutical industry.

## Supplementary Information

Supplementary information is available in the website <http://nopr.niscair.res.in/handle/123456789/58776>.

## Conflict of Interest

The authors declare that they have no conflict of interest

## Acknowledgement

The authors are thankful to the laboratory technicians of NMR and IR spectroscopy for their help, suggestions, and comments during the experimentation.

## References

- Piemontese L, Sergio R, Rinaldo F, Brunetti L, Perna F M, Santos M A & Capriati V, *Molecules*, 25 (2020) 574.
- Wechteti L, Mekni N H & Romdhani-Younes M, *Heterocycl Comm*, 24 (2018) 187.
- Rodriguez V, Pineda H, Ardila N, Insuasty D, Cardenas K, Roman J, Urrea M, Ramirez D, Fierro R, Rivera Z & Garcia J, *Int J Pept Res Ther*, 26 (2020) 585.
- Wechteti L, Mezni A & Romdhani-Younes M, *J Chem Bio Phy Sci Sec A*, 8 (2018) 154.
- Kumar S R & Leelavathi P, *J Mol Catal A Chem*, 266 (2007) 65.
- Ichikawa E I & Kato K, *Synthesis*, 1 (2002) 1.
- Coudures C, Pastor R, Szonyi S & Cambon A, *J Fluorine Chem*, 24 (1984) 105.
- Bergmeier S C, *Tetrahedron*, 56(2000) 2561.
- de Almeida C G, Reis S G, de Almeida A M, Diniz C G, da Silva V L & Hyaric M, *Chem Biol Drug Des*, 78 (2011) 876.
- Estolano-Cobián A, Noriega-Iribe E, Díaz-Rubio L, Padrón J M, Brito-Perea M, Cornejo-Bravo J M, Chávez D, Rivera R R, Quintana-Melgoza J M, Cruz-Reyes J & Córdova-Guerrero I, *Med Chem Res*, 29 (2020) 1986.
- Takehara J, Hashiguchi S, Fujii A, Inoue A & Ikariya T, *Chem Commun*, 22 (1996) 233.
- Kaptein B, Elsenberg H, Minnaard A J, Broxterman Q B, Hulshof L A, Koek J & Vries T R, *Tetrahedron Asymmetry*, 10 (1999) 1413.
- Solladié-Cavallo A, Lupattelli P, Bonini C & Bonis M D, *Tetrahedron Lett*, 44(2003) 5075.
- Porte A M, Reibenspies J & Burgess K, *J Am Chem Soc*, 120 (1998) 9180.
- Pimparkar K P, Miller D J & Jackson J E, *Ind Eng Chem Res*, 47 (2008) 7648.
- Liu C, Yin J, Xue J, Tao Y, Hu W & Zhang H, *Acta Tropica*, 182 (2018) 285.
- Calvert W J & Lefer D J, *Physiology (Bethesda)*, 28 (2013) 216.
- Baida A A, Rudakova A V & Agaev S G, *Russ J Phys Chem A*, 87 (2013) 243.
- Sengwa R J, Choudhary S & Bald A, *J Solut Chem*, 42 (2013) 1960.
- Kuz'min M V, Vasil'ev E P, Bagrov F V & Kol'tsov N I, *Int Polym Sci Technol*, 32 (2005) 32.
- Kuschel F, Hartmann L, Bauer M & Weissflog W, *Mol Cryst Liq Cryst*, 588 (2014) 51.
- Wu S, Snajdrova R, Moore J C, Baldenius K & Bornscheuer U T, *Angew Chem Int Ed*, 60 (2021) 88.
- Chennapuram M, Owolabi I A, Seki C, Okuyama Y, Kwon E, Uwai K, Tokiwa M, Takeshita M, Nakano H, *ACS Omega*, 3 (2018) 11718.
- Xu C, Xu J, Liu H & Li X, *Chin Chem Lett*, 29 (2018) 1119.
- Ullah V Z & Kim M, *Molecules*, 22 (2017) 547.
- Chu X Q, Ge D, Wang M L, Rao W, Loh T P & Shena Z L, *Adv Synth Catal*, 361 (2019) 4082.
- Souamti A, Kahlaoui M, Mohammed B, Diego-Gorrín A & Chehimi D B H, *Ceram Int*, 43 (2017) 10939.
- Souamti A, Lozano-Gorrin A D, Zayani L, Essayes S A, Abbassi M, Lalla E, Perez-Rodriguez C & Chehimi D B H, *J Electron Mater*, 45 (2016) 4418.
- Bejaoui A, Souamti A, Kahlaoui M, Lozano-Gorrin A D & Chehimi D B H, *Mater Sci Eng B*, 228 (2018) 224.
- Bejaoui A, Souamti A, Kahlaoui M, Lozano-Gorrin A D, Palomino J M & Chehimi D B H, *Mater Sci Eng B*, 240 (2019) 97.
- Souamti A, Kahlaoui M, Fezai R, Lozano-Gorrin A D & Chehimi D B H, *Mater Sci Eng B*, 244 (2019) 56.
- Souamti A, Kahlaoui M, Martin I R, Lozano-Gorrin A D, Lalla E & Chehimi D B H, *Mater Sci Eng B*, 247 (2019) Article 114384.
- A Souamti & Chehimi D B H, *Mater Sci Eng B*, 265 (2021) Article 115040.